

ORIGINAL ARTICLE

# CHK1 overexpression in T-cell acute lymphoblastic leukemia is essential for proliferation and survival by preventing excessive replication stress

LM Sarmiento<sup>1</sup>, V Póvoa<sup>1</sup>, R Nascimento<sup>2</sup>, G Real<sup>3,4</sup>, I Antunes<sup>1</sup>, LR Martins<sup>1</sup>, C Moita<sup>1</sup>, PM Alves<sup>3,4</sup>, M Abecasis<sup>5</sup>, LF Moita<sup>1</sup>, RME Parkhouse<sup>2</sup>, JPP Meijerink<sup>6</sup> and JT Barata<sup>1</sup>

Checkpoint kinase 1 (CHK1) is a key component of the ATR (ataxia telangiectasia-mutated and Rad3-related)-dependent DNA damage response pathway that protect cells from replication stress, a cell intrinsic phenomenon enhanced by oncogenic transformation. Here, we show that CHK1 is overexpressed and hyperactivated in T-cell acute lymphoblastic leukemia (T-ALL). *CHEK1* mRNA is highly abundant in patients of the proliferative T-ALL subgroup and leukemia cells exhibit constitutively elevated levels of the replication stress marker phospho-RPA32 and the DNA damage marker  $\gamma$ H2AX. Importantly, pharmacologic inhibition of CHK1 using PF-004777736 or CHK1 short hairpin RNA-mediated silencing impairs T-ALL cell proliferation and viability. CHK1 inactivation results in the accumulation of cells with incompletely replicated DNA, ensuing DNA damage, ATM/CHK2 activation and subsequent ATM- and caspase-3-dependent apoptosis. In contrast to normal thymocytes, primary T-ALL cells are sensitive to therapeutic doses of PF-004777736, even in the presence of stromal or interleukin-7 survival signals. Moreover, CHK1 inhibition significantly delays *in vivo* growth of xenotransplanted T-ALL tumors. We conclude that CHK1 is critical for T-ALL proliferation and viability by downmodulating replication stress and preventing ATM/caspase-3-dependent cell death. Pharmacologic inhibition of CHK1 may be a promising therapeutic alternative for T-ALL treatment.

*Oncogene* advance online publication, 18 August 2014; doi:10.1038/onc.2014.248

## INTRODUCTION

T-cell acute lymphoblastic leukemia (T-ALL) arises from transformed T-cell precursors carrying genetic lesions that block development and concomitantly promote self-renewal, proliferation and survival.<sup>1</sup> Current T-ALL treatment protocols involve aggressive chemotherapeutic strategies with considerable side effects,<sup>2</sup> fuelling the efforts to identify molecular players whose targeting selectively eliminates leukemia cells.

There is increasing evidence that oncogenes induce DNA replication stress, especially those that promote uncontrolled S-phase entry.<sup>3,4</sup> As loss of tumor suppressor genes encoding cell cycle inhibitors (such as cyclin dependent kinase 2a (CDKN2A)) and/or checkpoint mediators (such as ATM and TP53) occurs during the tumorigenic process, cancer cell integrity increasingly relies on mechanisms that afford protection against potentially catastrophic amounts of oncogene-induced replication stress. Disruption of CDKN2A/ARF and CDKN2B loci, and consequent inactivation of the cell cycle inhibitors p15 and p16<sup>ink4a</sup> occurs in most T-ALL cases.<sup>5,6</sup> NOTCH1 gain-of-function mutations are also frequent events in this malignancy<sup>7</sup> that promote CDK2 activity and cell cycle progression.<sup>8,9</sup> In addition, gain-of-function mutations in cytokine signaling elements<sup>10–12</sup> as well as microenvironmental cues such as interleukin-7 (IL-7) contribute to leukemia expansion by increasing the CDK activity and promoting S-phase entry.<sup>13</sup> Moreover, a specific oncogenetic subgroup has been identified in T-ALL that is associated with particularly high

expression of genes involved in cell cycle progression and mitosis.<sup>14</sup> These observations indicate that T-ALL cells may undergo intense proliferation, which potentiates replication stress.

Replication stress has been defined as the accumulation of recombinogenic stretches of single-stranded DNA (ssDNA) that most frequently derive from stalled replication forks.<sup>15</sup> DNA double-strand breaks trigger the ataxia telangiectasia-mutated-checkpoint 2 (ATM-CHK2) DNA damage response pathway,<sup>16</sup> whereas CHK1 is the downstream checkpoint kinase that conveys signals from ATM and Rad3-related (ATR) activation<sup>17</sup> that is exclusively engaged in response to exposed ssDNA.<sup>18</sup> The ATR/ATRIP (ATR-interacting protein) complex docks to RPA-coated ssDNA and promotes Rad17/Rad9-Rad1-Hus1(9-1-1)/TopBP1-dependent ATR activation and subsequent CHK1 phosphorylation, thereby fully activating the replication stress response (revised in refs<sup>16,18,19</sup>). In turn, CHK1 is involved in the intra-S-phase checkpoint by inhibiting the CDC25 family of phosphatases, and consequently the activation of S-phase CDKs.<sup>20</sup> In this way, CHK1 prevents replication fork collapse by inhibiting DNA replication origin firing<sup>21,22</sup> and favoring elongation from active replication forks,<sup>23</sup> whereas promoting the stability of stalled replication forks<sup>24</sup> and recruiting homologous DNA repair machinery components to damaged sites.<sup>25</sup>

In line with this role, CHK1 is expected to behave as a tumor suppressor. However, *CHEK1* loss-of-function mutations have not been found in human tumors,<sup>19</sup> in contrast to components of the

<sup>1</sup>Instituto de Medicina Molecular, Faculdade de Medicina, Universidade de Lisboa, Lisbon, Portugal; <sup>2</sup>Infections and Immunity Laboratory, Instituto Gulbenkian de Ciência, Oeiras, Portugal; <sup>3</sup>BET, Instituto de Biologia Experimental e Tecnológica, Oeiras, Portugal; <sup>4</sup>Instituto de Tecnologia Química e Biológica, Oeiras, Portugal; <sup>5</sup>Cardiologia Pediátrica Medico-Cirúrgica, Hospital Sta. Cruz, Carnaxide, Lisbon, Portugal and <sup>6</sup>Department of Pediatric Oncology/Hematology, Erasmus MC/Sophia Children's Hospital, Rotterdam, The Netherlands. Correspondence: Dr JT Barata, Instituto de Medicina Molecular, Faculdade de Medicina, Universidade de Lisboa, Av. Prof Egas Moniz, Lisbon 1649-028, Portugal. E-mail: joao\_barata@medicina.ulisboa.pt

Received 28 March 2014; revised 5 June 2014; accepted 26 June 2014

ATM-CHK2-p53 pathway. In addition, tissue-specific *Chek1* knock-out models do not support a role for CHK1 as a tumor suppressor,<sup>26,27</sup> and the expression of *Chek1* in a mouse transgenic model promotes oncogene-induced transformation through the inhibition of replication stress.<sup>15</sup> These studies suggest that CHK1 may facilitate tumorigenesis. In agreement, CHK1 is overexpressed in various human cancers.<sup>28–30</sup> Moreover, as CHK1-mediated checkpoint may protect tumor cells from the cytotoxic effects of chemotherapy, CHK1 inhibitors have been developed as chemosensitizers to enhance the cytotoxicity of DNA damage-inducing agents.<sup>31</sup> Recently, an extended version of this concept proposed that tumors with considerable amounts of intrinsic DNA damage, likely due to oncogene-induced replication stress, would be particularly sensitive to the inhibition of the ATR-CHK1 axis,<sup>18</sup> a concept still poorly explored.

Here, we show that T-ALL cells display noticeable levels of replication stress markers with concomitant CHK1 overexpression and hyperactivation. *CHEK1* transcript levels are especially elevated in patients of the proliferative T-ALL subgroup, suggesting that CHK1 may protect leukemia cells from increased replication stress resulting from uncontrolled cell cycle progression. Furthermore, we provide evidence that CHK1 is critical for T-ALL cell viability by decreasing replication stress and preventing ATM/caspase-3-dependent apoptotic death. We also present evidence that CHK1 pharmacologic inhibition is a novel, promising therapeutic option for T-ALL treatment.

## RESULTS

### T-ALL cells overexpress *CHEK1*

Given the importance of *Chk1* to the survival of murine T-cell progenitors<sup>27</sup> and the growing evidence that CHK1 is overexpressed in cancer cells,<sup>28–30</sup> we hypothesized that CHK1 could be abnormally expressed in T-ALL. We thus compared the levels of *CHEK1* transcript in leukemia cells from diagnostic pediatric T-ALL patients with those in normal human thymocytes. Real-time PCR analysis revealed that 60% of primary T-ALL samples (Figure 1a) and all human T-ALL cell lines tested (Figure 1b) expressed higher levels of *CHEK1* mRNA than thymocytes. The average expression of *CHEK1* mRNA was ~4-fold higher in primary T-ALL cells and ~10-fold higher in T-ALL cell lines than in normal thymocytes (Figure 1c). Notably, *CHEK1* transcript levels within the main normal thymocyte sub-populations were higher in the CD4<sup>+</sup>CD8<sup>+</sup> double-positive stage (Supplementary Figure 1), which is highly enriched in precursors undergoing proliferation upon  $\beta$ -selection.<sup>2</sup> We further analyzed *CHEK1* expression in a previously described microarray data set of a large pediatric T-ALL cohort.<sup>14</sup> Similar to our initial results (Figure 1a), we found that ~50% of T-ALL patients expressed two- to eightfold higher levels of *CHEK1* mRNA, and that, overall, T-ALL cells displayed significantly higher *CHEK1* transcript levels than healthy controls (Figure 1d). Interestingly, *CHEK1* levels varied among different T-ALL subgroups<sup>14</sup>

(Figure 1d). *CHEK1* expression was higher in the proliferative and TAL-LMO subgroups than in the TLX or ETP-ALL (Figure 1d). Moreover, the subgroup within the TAL-LMO cluster with higher expression of cell cycle regulatory genes, namely CDK1/*CDC2*,<sup>14</sup> presented higher *CHEK1* levels than the remaining TAL-LMO cases (Figure 1e).

T-ALL cells present elevated markers of DNA damage and replication stress, and display ATR/CHK1 pathway constitutive activation

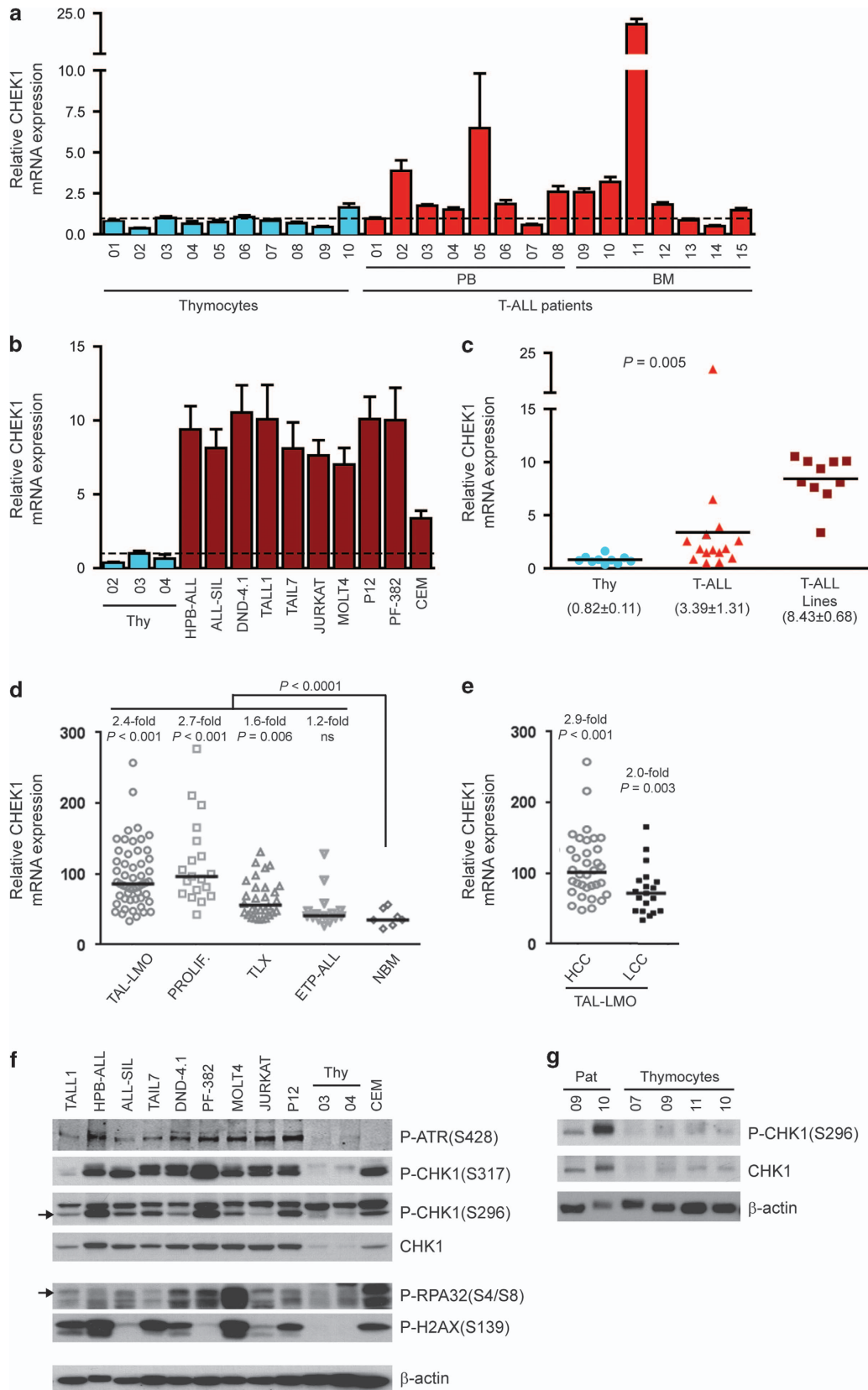
Next, we wondered whether the increased *CHEK1* expression translated into protein levels and associated with activation of the ATR/CHK1-replicative stress response pathway. Immunoblot analysis showed that 9 of 10 T-ALL cell lines (Figure 1f) and both T-ALL patient samples analyzed (Figure 1g) displayed elevated levels of CHK1 protein when compared with normal thymocytes. Moreover, we found that these T-ALL cell lines also exhibited increased Ser317 CHK1 phosphorylation, a marker of CHK1 activation by ATR, and elevated levels of activated ATR measured by Ser428 phospho-ATR (Figure 1f). Notably, evaluation of CHK1 autophosphorylation residue (Ser296), which reflects CHK1 kinase activity as it is phosphorylated by CHK1 itself, demonstrated that all T-ALL cell lines (Figure 1f) and primary patient cells (Figure 1g) presented constitutive CHK1 activity, whereas only trace amounts of this form were detected in normal thymocytes (Figures 1f and g). Consistent with CHK1 activation, T-ALL cells displayed increased levels of the replication stress marker P-RPA32 and of the DNA damage marker  $\gamma$ H2AX (Figure 1f).

Pharmacologic inhibition of CHK1 promotes death and impairs proliferation of T-ALL cells in a dose- and time-dependent manner. It has been proposed that cancer cells presenting intrinsic elevated replication stress rely on activation of the ATR/CHK1 pathway to restrain the accumulation of deleterious levels of DNA damage.<sup>18</sup> The corollary is that cancer cells with elevated replication stress may be particularly sensitive to ATR and CHK1 inhibition. We therefore assessed the effects of the CHK1 pharmacologic inhibitor PF-00477736 on T-ALL cell viability and proliferation. We found that all the T-ALL cell lines tested were highly sensitive to PF-00477736 treatment in the low nanomolar range, with half-maximum inhibitory concentration (IC<sub>50</sub>) values varying between 20 and 109 nM (Figure 2a). Furthermore, PF-00477736 induced cell death in a dose- and time-dependent manner in T-ALL cell lines, and a drug concentration of ~3 times the IC<sub>50</sub> eliminated more than 90% of cells in 72 h (Figure 2b and Supplementary Figure 2). We also confirmed that the decrease in viability was paralleled by an equivalent reduction in proliferation (Figure 2c and Supplementary Figure 2). As expected, the ATR inhibitor ETP-46464<sup>32</sup> also induced T-ALL cell death in a concentration-dependent manner (Supplementary Figure 3).

**Figure 1.** T-ALL cells display constitutive CHK1 activation and DNA damage. **(a and b)** Expression of *CHEK1* mRNA determined by quantitative real-time PCR in T-ALL primary samples **(a)** and in T-ALL cell lines **(b)** compared with that of normal thymocyte samples. Values are mean  $\pm$  s.e.m. of triplicate. **(c)** *CHEK1* mRNA levels of normal thymocytes ( $n = 10$ ), primary T-ALL cells ( $n = 15$ ) and T-ALL cell lines ( $n = 10$ ). Points represent individual samples, horizontal bars denote mean and mean  $\pm$  s.e.m. is shown within parentheses. **(d and e)** *CHEK1* mRNA expression data extracted from the microarray analysis of 117 pediatric T-ALL samples of the COALL and DCOG patient cohorts, subjected to a Kruskal–Wallis comparative analysis of the indicated T-ALL molecular subgroups, defined by unsupervised cluster analysis as in Homminga *et al.*,<sup>14</sup> against a control group (seven normal bone marrow samples). Points represent individual samples, horizontal bars denote mean and the fold change from the control group is indicated on top of each T-ALL subgroup. **(e)** The TAL-LMO cluster is further divided into cases that express high (HCC), proliferative-like or low (LCC) levels of cell cycle genes. **(f and g)** Cell lysates of T-ALL cell lines **(f)** or primary leukemia cells **(g)** and normal human thymocytes **(f and g)** were immunoblotted with the indicated phospho-specific antibodies against ATR and CHK1 or the DNA damage and replication stress markers, H2AX and RPA32, respectively, or antibodies against total CHK1 or actin as the loading control. Arrows discriminate the serine 296 phospho-CHK1 band and the hyperphosphorylated (serine 4/serine 8) form of RPA32 from unspecific background bands. Normal human thymocytes are denoted as 'Thy' in panels **b, c** and **f**.

T-ALL cell death after CHK1 inactivation associates with a block in replication and induction of apoptosis  
We next examined the cellular mechanisms underlying the loss of viability and proliferation upon CHK1 inhibition in T-ALL cells.

CHK1 inactivation has been associated with aberrant cell cycle progression owing to increased replication fork stalling and collapse. Using three T-ALL cell lines with different sensitivities to PF-00477736, we found that CHK1 inhibition profoundly altered



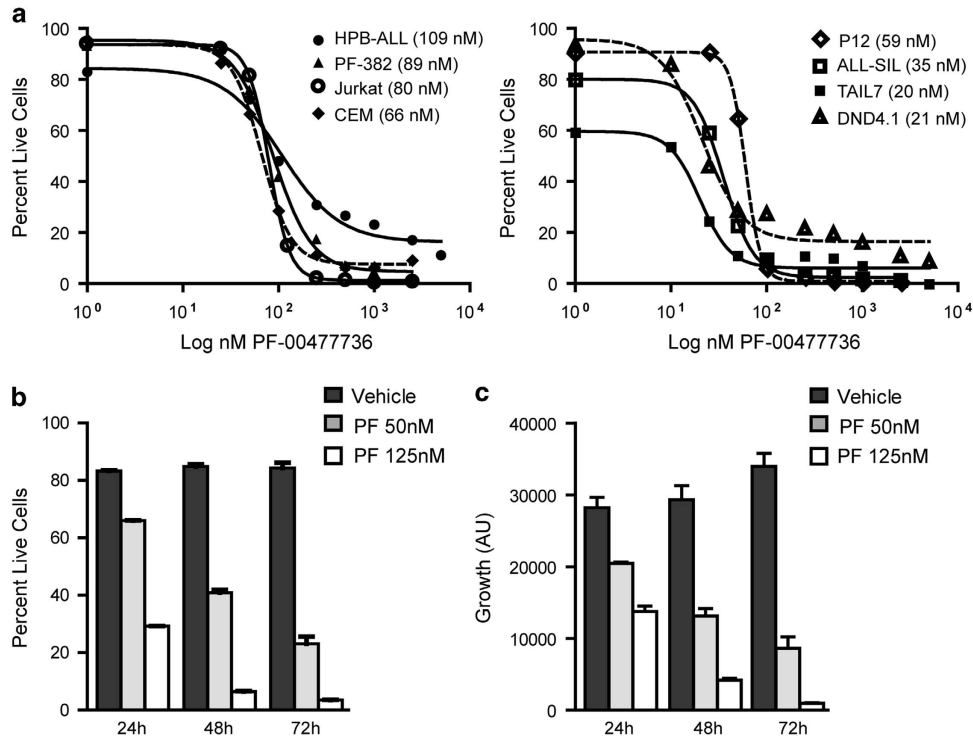


**Figure 2.** T-ALL cell lines are sensitive to CHK1 pharmacologic inhibition. **(a)** Dose–response curves of the CHK1-specific inhibitor PF-00477736 in eight T-ALL cell lines. The IC<sub>50</sub> is indicated within parenthesis. Percentage of live cells was determined by flow cytometry discrimination of physical parameters (FSC × SSC) upon incubation of cells with PF-00477736 for a period of time equivalent to the doubling time of each cell line (48 h for all T-ALL cell lines except the primary-like TAIL7 cells, which were cultured for 144 h). **(b and c)** Time-dependent response to the indicated doses of PF-00477736 of one representative T-ALL cell line (ALL-SIL) regarding viability **(b)**, as measured by the percentage of live cells identified by FSC × SSC flow cytometry analysis, and proliferation **(c)**, as measured by Alamar blue assay and indicated in arbitrary units. Values are mean ± s.d.

cell cycle progression (Figure 3a). PF-00477736 treatment led to the accumulation of T-ALL cells with intermediate  $2n-4n$  DNA content that was evident by 24 h, indicating impaired replication progression (Figure 3a). Moreover, the G2/M checkpoint was abrogated upon CHK1 inhibition, as determined by the down-regulation of CDK1 phospho-Tyr15 and accumulation of hyperphosphorylated CDC25C (Figure 3b), which reflects CDK1 activation and stabilization of CDC25C mitotic form.

Impaired replication combined with the loss of the CHK1-dependent G2/M checkpoint appears to drive cells with incompletely replicated DNA into premature entry in mitosis resulting in apoptosis.<sup>19</sup> We thus wondered whether these cell cycle alterations associated with apoptosis of T-ALL cells after CHK1 inactivation. We observed that PF-00477736 consistently augmented the percentage of apoptotic cells at IC<sub>50</sub> concentrations (Figure 3c) as well as in a dose-dependent manner (Figure 3d), confirming that CHK1 inhibition induced T-ALL apoptotic cell death. Notably, similar results were obtained upon short hairpin RNA (shRNA)-mediated *CHEK1* depletion in Jurkat cells that accumulated with intermediate  $2n-4n$  DNA content (Figure 3e) and underwent apoptosis (Figure 3f).

CHK1 inactivation results in high levels of replication stress and the induction of the ATM-CHK2 DNA damage response pathway in T-ALL cells

Next, we sought to characterize the molecular players associated with the replication block triggered by the loss of CHK1. RPA is recruited to ssDNA at stalled and collapsed replication forks and RPA phosphorylation is important for checkpoint activation during replication stress.<sup>33,34</sup> Histone-2AX phosphorylation at Ser139

( $\gamma$ H2AX) is enhanced in CHK1-depleted cells undergoing replication stress<sup>35,36</sup> and it can be used to monitor replication stress-induced DNA damage.<sup>34</sup> Indeed, we found that *CHEK1* silencing or CHK1 pharmacologic inhibition, confirmed by Ser296 phospho-CHK1 downregulation, resulted in a striking upregulation of phospho-RPA32 and  $\gamma$ H2AX (Figures 4a and b and Supplementary Figure 4). Moreover, the increase in  $\gamma$ H2AX levels in PF-00477736-treated T-ALL cells correlated with the appearance of nuclei with multiple (> 10) intense foci or pan-nuclear  $\gamma$ H2AX immunofluorescence staining (Figure 4c and Supplementary Figure 4), a distinct feature of replication stress.<sup>36</sup> These observations indicate that constitutive CHK1 activity is mandatory to prevent excessive replication stress that is intrinsically associated with proliferation in T-ALL cells.

The increase in  $\gamma$ H2AX associated with the loss of CHK1 has been documented to depend on endonuclease processing of collapsed replication forks into DNA double-strand break.<sup>35</sup> Therefore, we examined possible changes in the activation of ssDNA and DNA double-strand break damage response pathways (ATR/CHK1 and ATM/CHK2, respectively) upon CHK1 loss. We first confirmed that ATR and CHK1 were activated in T-ALL cells, as denoted by high basal levels of Ser428 phospho-ATR and Ser317 phospho-CHK1. In contrast, we did not find evidence of constitutive ATM/CHK2 activation, as measured by the phosphorylation levels of the ATM target residues Thr68 on CHK2 and Ser1981 on ATM itself (Figures 4a and b and Supplementary Figure 4). CHK1 inhibition or knockdown resulted in the down-regulation of Ser428 phospho-ATR, indicating reduced ATR activation, whereas Ser1981 phospho-ATM and Thr68 phospho-CHK2 were upregulated (Figures 4a and b and Supplementary Figure 4). In agreement, Ser317 and Ser345 phospho-CHK1 were

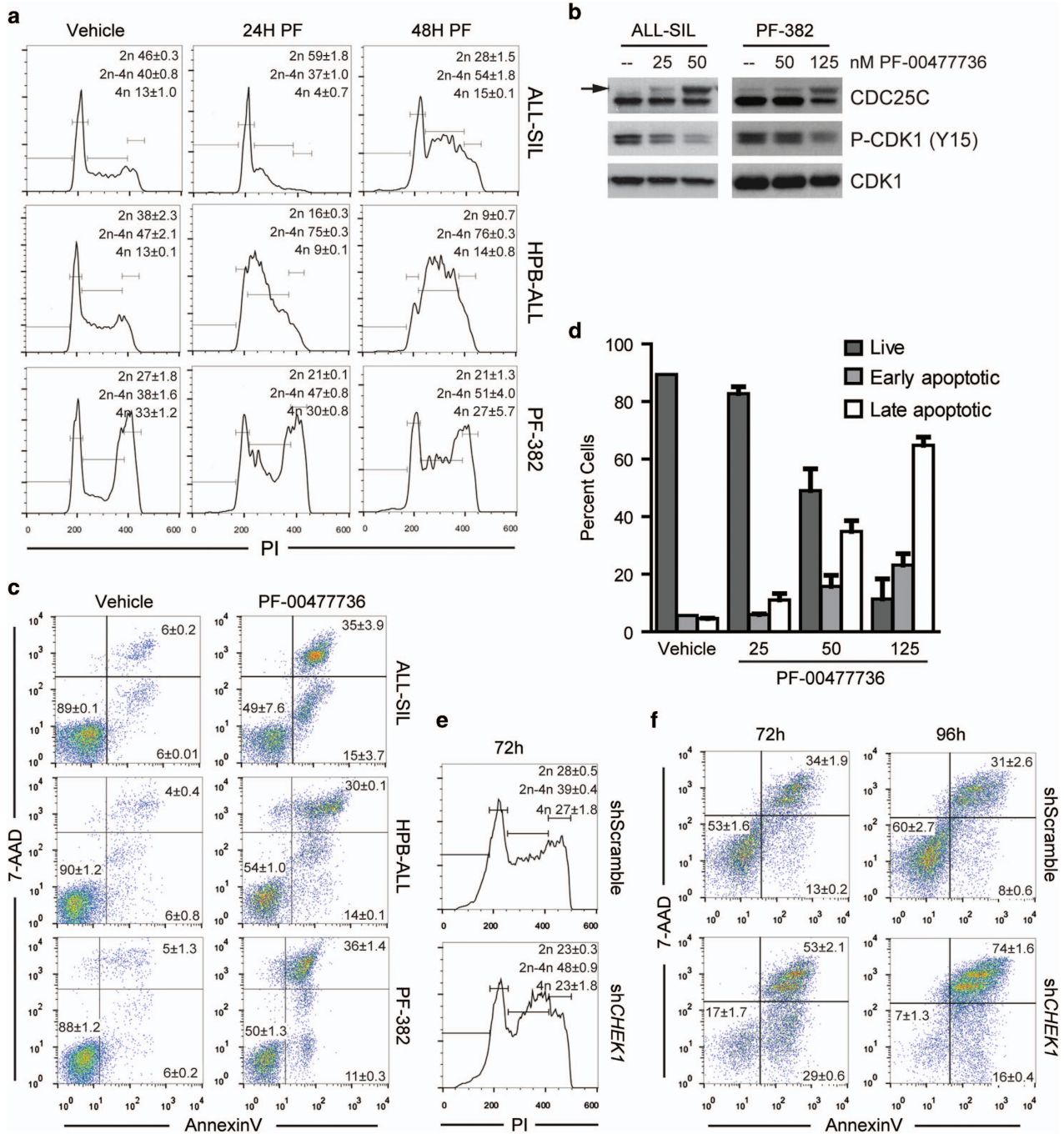


**Figure 3.** CHK1 inactivation causes replication arrest and apoptosis in T-ALL cell lines. **(a)** Representative flow cytometry histograms of propidium iodide (PI)-stained DNA of ALL-SIL, HPB-ALL and PF-382 T-ALL cells after 24 and 48 h of treatment with PF-0047736 doses in the IC<sub>50</sub> range (50, 125 and 125 nM, respectively). Indicated gates define the percentage of diploid (2n), replicating (2n-4n) and tetraploid (4n) cells. Data are representative of 2 independent experiments and values represent the mean ± s.d. of triplicates. **(b)** Lysates of ALL-SIL and PF-382 T-ALL cells treated for 48 h with IC<sub>50</sub> doses of PF-00477736 immunoblotted with antibodies against CDC25C or tyrosine 15 phospho-CDK1 or total CDK1 as the loading control. The arrow indicates the 70 kDa hyperphosphorylated mitotic form of CDC25C that accumulates upon treatment with PF-00477736. **(c)** Representative flow cytometry dot plots of annexin-V/7-AAD staining showing the decrease in live cells (annexin-V<sup>-</sup>/7-AAD<sup>-</sup>) and increase in early apoptotic (annexin-V<sup>+</sup>/7-AAD<sup>-</sup>) and late apoptotic/necrotic (annexin-V<sup>+</sup>/7-AAD<sup>+</sup>) ALL-SIL, HPB-ALL and PF-382 cells caused by CHK1 inhibition upon a 48 h treatment with doses of PF-00477736 in the IC<sub>50</sub> range. Values represent the mean ± s.d. of the cell percentage within each quadrant. **(d)** Dose-dependent induction of apoptosis by PF-00477736 in ALL-SIL cells after 48 h of treatment as determined by flow cytometry analysis of annexin-V/7-AAD staining. Columns denote the mean and s.d. for each condition. **(e and f)** Cell cycle and apoptosis of Jurkat cells transduced with scramble or CHEK1-targeting shRNA. **(e)** DNA distribution histograms 72 h posttransduction showing the accumulation of cells with partially replicated 2n-4n DNA, and **(f)** annexin-V/7-AAD dot plots showing increased apoptosis at 72 and 96 h posttransduction, caused by CHEK1 knockdown. Data are representative of two independent experiments and values represent mean ± s.d. of triplicates.

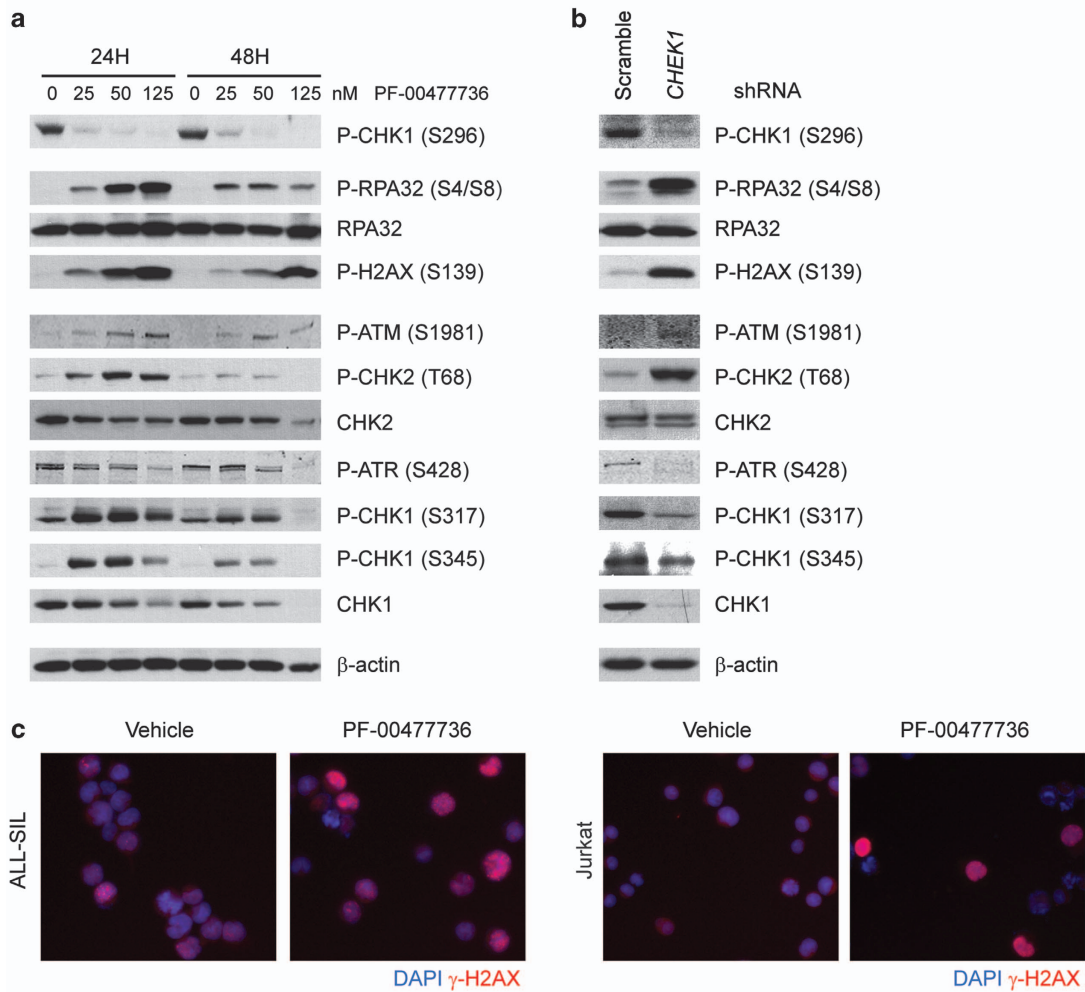


**Figure 4.** CHK1 inactivation induces replication stress and activates the ATM-CHK2 double-strand break pathway. **(a)** ALL-SIL cells were incubated with various doses of PF-00477736 for the indicated time points and immunoblotted with the indicated antibodies. **(b)** Jurkat cells expressing scramble or *CHEK1*-targeting shRNAs were collected at 72 h and immunoblotted with the indicated antibodies. Actin was used as loading control in both instances. **(c)** Representative immunofluorescence images of serine 139 phospho-H2AX ( $\gamma$ H2AX) showing a pan-nuclear distribution in ALL-SIL (left panels) and Jurkat (right panels) cells treated for 48 h with 25 and 50 nM of PF-00477736, respectively, as compared with vehicle- (dimethylsulfoxide, DMSO) treated cells.

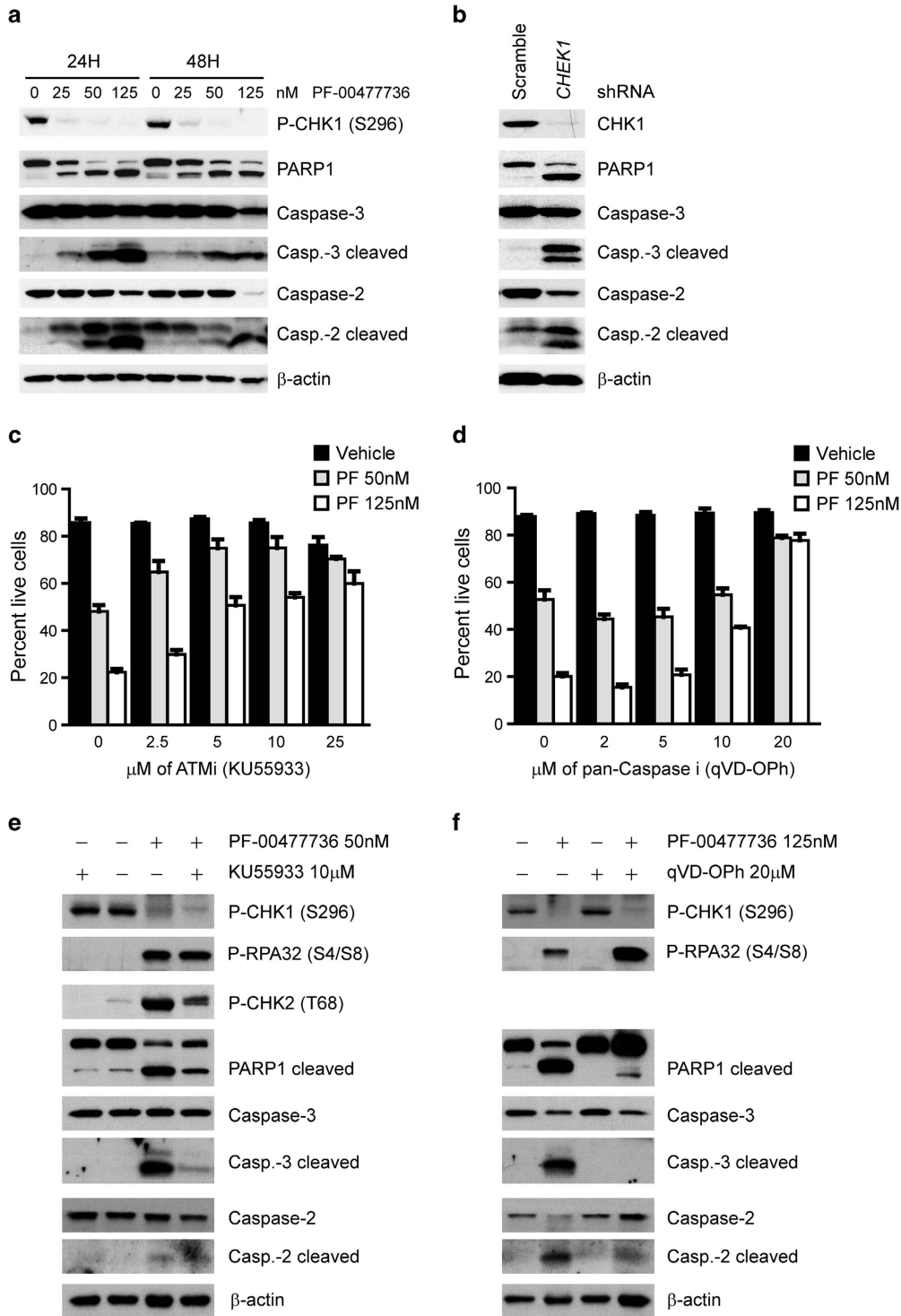
increased upon CHK1 inhibition (Figure 4a) in an ATM- rather than in an ATR-dependent manner (data not shown). However, high doses or longer exposure to PF-00477736 led to the down-regulation of total CHK1, suggesting that high levels of DNA damage-induced CHK1 phosphorylation lead to CHK1 degradation in T-ALL cells, as observed also in other contexts.<sup>37</sup> Overall, these data indicate that loss of CHK1 drives the accumulation of DNA damage caused by intrinsic replication stress, resulting in the activation of the ATM/CHK2 pathway and ATM-dependent upregulation of CHK1 phosphorylation in T-ALL, independently of the ATR status.

ATM and caspase activity are required for apoptosis induced by CHK1 inactivation in T-ALL cells

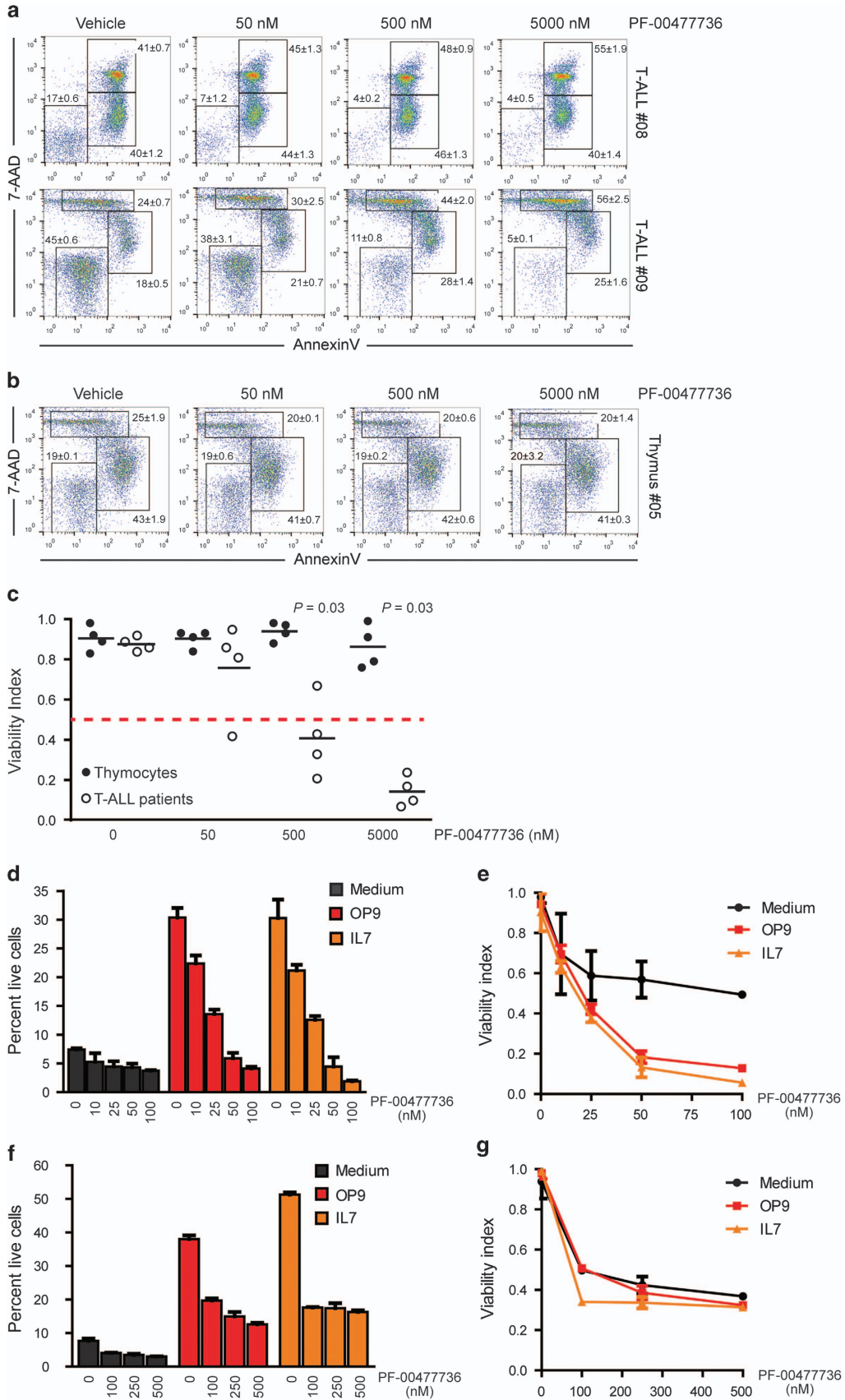
Next, we characterized the molecular players engaged in the apoptotic response that resulted from excessive replication stress after CHK1 inactivation in T-ALL cells. CHK1 has been reported as a key suppressor of apoptotic pathways, namely those involving caspase-2<sup>38</sup> and caspase-3.<sup>39</sup> Immunoblot analysis showed that apoptosis upon PF-00477736 treatment or *CHEK1* depletion was paralleled by the cleavage of poly (ADP-ribose) polymerase 1,

caspase-3 and caspase-2 (Figures 5a and b and Supplementary Figure 4). Given the importance of ATM in the induction of caspase-2 cleavage<sup>38</sup> and because CHK1 inhibition led to ATM activation in T-ALL cells, we questioned whether ATM was involved in the apoptotic process triggered by CHK1 inactivation in T-ALL. We found that the ATM inhibitor KU55933 rescued the viability of PF-00477736-treated ALL-SIL cells in a dose-dependent manner (Figure 5c). T-ALL cells were also rescued using the pancaspase inhibitor qVD-Oph (Figure 5d).

At the molecular level, we confirmed that ATM was efficiently inhibited by KU55933, as observed by the reduction in Thr68 phospho-CHK2 (Figure 5e). ATM inhibition resulted in a substantial decrease in the cleavage of poly (ADP-ribose) polymerase 1 and caspase-3, but not caspase-2, without affecting PF-00477736-induced P-RPA32 (Figure 5e), whereas qVD-OPH completely abolished caspase-3 activation and significantly reduced caspase-2 and poly (ADP-ribose) polymerase 1 cleavage (Figure 5f). Overall, these data suggest that ATM and caspases, particularly caspase-3, are recruited following replication stress-induced DNA damage to induce apoptosis in T-ALL cells when CHK1 activity is compromised.



**Figure 5.** ATM and caspase-3 are required for apoptosis induced by CHK1 inactivation in T-ALL cells. **(a)** ALL-SIL cells were incubated with PF-00477736 for the indicated time points and immunoblotted with the indicated antibodies. **(b)** Jurkat cells were transduced with scramble or *CHEK1* shRNAs and analyzed at 72 h and immunoblotted with the indicated antibodies. Actin was used as loading control in both instances. **(c and d)** Percentage of live cells determined by FSC × SCC flow cytometry discrimination in ALL-SIL cells pretreated for 2 h with vehicle (dimethylsulfoxide, DMSO), or various doses of the ATM inhibitor KU55933 **(c)** or the pancaspase inhibitor qVD-Oph **(d)**, and subsequently cultured for 24 h upon adding 50 or 125 nM of the CHK1 inhibitor PF-00477736. **(e and f)** Lysates of ALL-SIL cells pretreated for 2 h with vehicle (–) or the indicated doses of KU55933 **(e)** or qVD-Oph **(f)**, and subsequently cultured for 24 h upon the addition of the indicated doses of PF-00477736 were immunoblotted with the indicated antibodies. P-CHK1 S296 was used as a measure of CHK1 kinase activity, P-CHK2 Thr68 as a measure of ATM kinase activity and actin as the loading control.



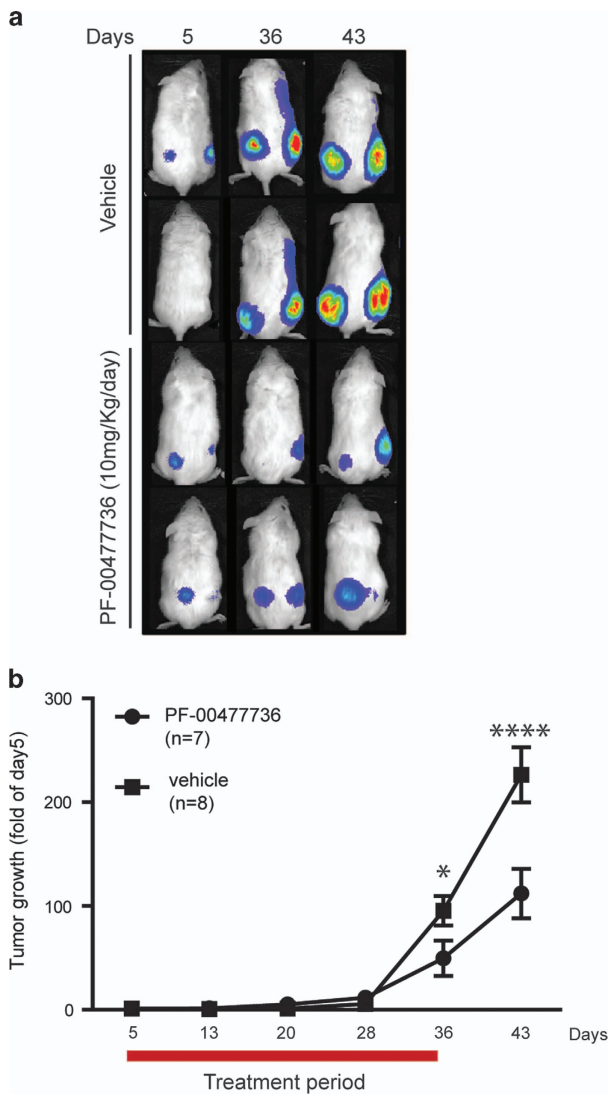


**Figure 7.** PF-00477736 delays T-ALL tumor growth *in vivo*. Non-obese diabetic/severe-combined immunodeficiency (NOD/SCID) mice were injected subcutaneously with  $10^7$  DND-4.1.Luc.GFP cells in each flank. Five days after cell transfer, mice were equally distributed according to the tumor burden into two groups: control (vehicle,  $n=8$ ) and PF-00477736-treated (10 mg/kg, *i.p.*, daily,  $n=7$ ). **(a)** Bioluminescence images at days 5, 36 and 43 after xenotransplant of two representative mice were selected from each group. **(b)** Detailed longitudinal analysis of tumor burden progression. The red bar indicates treatment duration (from day 5 to day 35 inclusive). Data indicate mean  $\pm$  s.e.m. of tumor burden (bioluminescence signal) normalized for each mouse tumor burden evaluated at day 5; \* $P < 0.05$  and \*\*\*\* $P < 0.0001$  (two-way analysis of variance).

CHK1 pharmacologic inhibition using PF-00477736 is cytotoxic to primary T-ALL patient cells

To evaluate the potential clinical applicability of our observations, we next assessed the sensitivity of primary T-ALL leukemia samples to PF-00477736. Analysis of Annexin-V/7-aminoactinomycin D (7-AAD) revealed that PF-00477736 significantly enhanced the spontaneous apoptosis of *ex vivo* cultured primary T-ALL cells in a dose-dependent manner (Figures 6a and c), whereas it did not alter that of normal thymocytes (Figures 6b and c). *In vivo*, leukemia cells are exposed to cues from the tumor microenvironment, including cell-to-cell contact and trophic signals, such as IL-7.<sup>40–44</sup> Therefore, we evaluated whether the loss of viability induced by PF-00477736 in primary T-ALL cells could be altered by exposure to OP9 coculture or IL-7 stimuli. As expected, both stromal cell coculture and IL-7 stimulation promoted primary T-ALL cell survival (Figures 6d and f and Supplementary Figure 5). However, PF-00477736 treatment clearly reversed this effect, with a dose-dependent tendency to reduce leukemia cell viability to levels that were similar to, or even below, those observed in the medium alone (Figures 6d–g and Supplementary Figure 5). Notably, T-ALL patient no. 10 who presented the highest levels of Ser296 phospho-CHK1 (Figure 1g) displayed the highest sensitivity to PF-00477736, specifically in the presence of exogenous stimuli (Figures 6d and e). Overall, these results demonstrate that primary T-ALL cells can be selectively eliminated by therapeutic doses of the CHK1 inhibitor PF-00477736. This effect appears to be maintained, or even potentiated, in the presence of environmental cues and to correlate with the levels of CHK1 activity.

CHK1 inhibitor PF-00477736 restrains T-ALL growth *in vivo*

To further explore the therapeutic potential of CHK1 inhibition, we next used a mouse subcutaneous xenotransplantation model of human T-ALL to assess whether systemic administration of PF-00477736 could limit leukemia growth *in vivo*. Longitudinal follow-up of treatment response demonstrated that PF-00477736 significantly reduced T-ALL tumor growth (Figure 7). This effect was perceptible as soon as the engraftment became evident, by day 36 ( $P < 0.05$ ), and was striking at day 43 ( $P < 0.0001$ ), at which time the mice were not receiving treatment any longer and were humanely killed. These results support the contention that CHK1 targeting may be a novel, feasible strategy worth including in the arsenal against T-ALL.

## DISCUSSION

Oncogene-induced replication stress triggers CHK1 activation via the ATR-dependent DNA damage response pathway. While the function of CHK1 as a cell cycle checkpoint kinase suggests it should have an antitumor role, there is evidence that the opposite may be true in at least some cancers.<sup>29,30,45</sup> This likely relates to the fact that CHK1 protects cells from the deleterious effects of replication stress, whose potential to trigger cell death increases

**Figure 6.** T-ALL patient cells but not normal thymocytes are sensitive to CHK1 inhibition. **(a and b)** Annexin-V/7-AAD flow cytometry dot plots of two representative T-ALL patients (no. 08, top and no. 09, bottom) **(a)** and one representative thymocyte sample (no. 05) **(b)** treated with the indicated doses of PF-00477736 for 72 and 96 h, respectively. Values indicate the mean  $\pm$  s.d. of the cell percentage gated within each quadrant. **(c)** Viability index, determined by FSC  $\times$  SSC flow cytometry discrimination, of four T-ALL patients (nos. 06, 07, 08 and 09) compared with four thymocyte samples (no. 05, 12, 13 and 14) treated with the indicated doses of PF-00477736. Points represent individual samples and horizontal bars denote mean ( $P < 0.05$ ; two-tailed Student's *t*-test). **(d–g)** Percentage of live cells **(d and f)** and viability index **(e and g)** of two T-ALL patient samples (no. 10, **d** and **e** and no. 08, **f** and **g**) cultured in medium alone, medium supplemented with hIL-7 (10 ng/ml) or cocultured with an OP9 stromal layer, and exposed to dimethylsulfoxide (DMSO), as vehicle control (indicated as 0 nM PF-00477736), or to the indicated doses of PF-00477736 for 72 h. In these conditions, PF-00477736 did not alter the morphology and viability of OP9 cells (not shown). Data points denote mean and s.d. of triplicate of representative experiments.

as cancer develops. Hence, there may be a selective pressure for CHK1 activation during tumorigenesis. Here, we provided evidence that this is the case in T-ALL, where CHK1 appears to have an oncogene-like function. First, we demonstrated that CHK1 is overexpressed and constitutively activated in T-ALL cell lines and primary patient samples. This is consistent with the high basal levels of replication stress we identified in T-ALL cells. These levels were nonetheless within an acceptable range to the normal function of leukemia cells, as activity of the ATR-CHK1 axis restrained excessive replication stress and consequent cell collapse (Figure 8). This was demonstrated by the fact that CHK1 inactivation resulted in the accumulation of cells with incompletely replicated DNA, increased DNA damage, ensuing ATM/CHK2 activation and subsequent ATM- and caspase-3-dependent apoptosis (Figure 8). Consequently, CHK1 inactivation led to leukemia cell death *in vitro*, even in the presence of survival stimuli, and significantly delayed leukemogenesis *in vivo*. In agreement with this model, pharmacologic inhibition of ATR resulted also in T-ALL cell death.

Why did T-ALL cells die upon CHK1 inactivation? Loss of CHK1 function has been linked to replication stress overload<sup>18</sup> and induction of apoptosis<sup>30,45</sup> with mitotic catastrophe occurring in cells that underwent unscheduled mitotic entry with incompletely replicated DNA.<sup>19,45,46</sup> Thus, the most likely explanation is that death by mitotic catastrophe<sup>47</sup> ensued blockade of CHK1 in T-ALL cells. Despite no obvious increment of cells with a DNA content typical of G2/M (4n), we found a clear decrease in the inhibitory phosphorylation of CDK1 at Tyr15 upon CHK1 inhibition, accompanied by the upregulation of the mitotic form of CDC25C. These observations indicate that CHK1 inhibition resulted in the expected impairment of the G2/M checkpoint, which, in turn, should allow T-ALL cells with incompletely replicated DNA to enter mitosis aberrantly, triggering mitotic catastrophe. This possibility is further supported by our findings of caspase-2 and caspase-3 activation and of the requirement for ATM activity, as has been documented to occur during mitotic catastrophe.<sup>46,47</sup> Moreover, CHK1 has been reported as a key suppressor of the ionizing radiation-induced, ATM-dependent caspase-2 cleavage<sup>38</sup> and of death induced by replication inhibitors via caspase-3 activation.<sup>39</sup> Our data indicate that ATM and caspase-3 are mandatory for apoptosis of T-ALL cells upon replication stress and overt DNA damage that arise at early time points (up to 24 h) after CHK1 inhibition. It should be noted, however, that PF-00477736-treated

leukemia cells eventually die at later time points, even in the presence of ATM or caspase inhibitors (data not shown). This suggests that, whereas T-ALL apoptosis by loss of CHK1 relies on ATM and caspase-3 activation, other molecular players, such as DNA-PKc (which we hypothesize is responsible for Ser4/8 phosphorylation of RPA32 when ATM is inhibited<sup>34</sup>), are capable of leading T-ALL cells to death. Furthermore, our experiments do not exclude a role for caspase-2 as a late driver of apoptosis, as caspase-2 activation was not dependent on ATM, and the highest tolerable dose of qVD-OPh failed to fully prevent caspase-2 cleavage. Ultimately, non-apoptotic (i.e. caspase-independent) pathways may participate in T-ALL cell death induced by CHK1 inhibition.

CHK1 inhibitors have been shown in preclinical settings to potentiate the effect of or override resistance to antitumor agents,<sup>19,31</sup> and transited to clinical trials with these goals.<sup>31,48</sup> In T-ALL, agents such as 7-hydroxystaurosporine (UCN-01) or geldanamycin, which negatively modulate CHK1 activity, were previously used in combination with drugs such as doxorubicin<sup>49</sup> or with signaling-specific inhibitors<sup>50</sup> to induce apoptosis in cell lines. Our studies constitute the first demonstration that CHK1 inactivation *per se*, using a highly selective inhibitor<sup>51</sup> or gene silencing, drives T-ALL cell death. Our results are in line with the recent demonstration that CHK1 inhibitors could be efficient as single agents in eliminating neuroblastoma and melanoma cells.<sup>30,45</sup>

Importantly, CHK1 inhibition did not significantly affect normal human thymocytes cultured *in vitro*, nor did it induce any evident toxicities in treated mice. Given that a majority of T-ALL cases overexpressed CHK1 and T-ALL cells were sensitive to CHK1 inactivation, these observations open a new therapeutic window for the possible clinical testing of CHK1 small-molecule inhibitors in this malignancy. However, it should be noted that CHK1 and ATR are essential for cell viability during early embryonic development<sup>17,52</sup> and for proliferating adult mouse cells,<sup>26,27</sup> namely T-cell progenitors.<sup>27</sup> Nonetheless, our evidence that T-ALL cells express more activated CHK1 than freshly collected thymocytes supports the notion that leukemic cells may be considerably more dependent on CHK1 for survival and therefore selectively susceptible to low doses of inhibitor, which would spare T-ALL normal counterparts.

Our molecular data suggested that CHK1 inhibitor drugs may be valid therapeutic tools in T-ALL. As proof of concept, we tested the effect of PF-00477736 on primary leukemia samples and showed that all five patients analyzed displayed sensitivity to the small-molecule inhibitor at doses below 500 nM, very close to the biologic concentration defined to suppress CHK1 activity with high selectivity.<sup>51</sup> Interestingly, the four patients that were more sensitive to PF-00477736 expressed higher levels of CHK1 mRNA than the least responsive patient (no. 7), which displayed similar transcript levels to those of normal thymocytes. Moreover, the patient who was most sensitive to the lower doses of PF-00477736 (no. 10) not only displayed the highest levels of mRNA but also strikingly higher levels of CHK1 protein and activity. Although the low number of T-ALL cases we were able to analyze precludes proper evaluation of associations between CHK1 expression/activity and sensitivity to CHK1 antagonists, these observations are noteworthy and should propel further investigation allowing for the characterization of those patients who could benefit the most from treatment with CHK1 inhibitors. Also of note, the preliminary results obtained with the human T-ALL xenotransplantation model reinforce the potential clinical interest of CHK1 inhibitors to treat T-ALL, particularly taking into account that the short treatment period we adopted may have led to an underestimation of the anti-leukemia impact of CHK1 inactivation. From a therapeutic standpoint, it is also worth considering the potential of such inhibitors in eradicating T-cell leukemia stem cells, particularly when located in niches that stimulate their proliferation. Moreover, in light of recent evidence that T-cell leukemia stem cells are

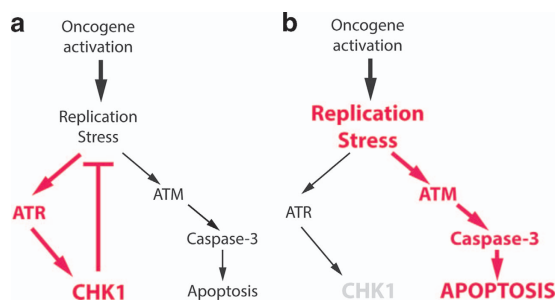


**Figure 8.** Model for CHK1 function, and loss of viability induced by CHK1 inactivation, in T-ALL. **(a)** T-ALL cells display the potential to generate high levels of replication stress (RS) from intrinsic origin (i.e. driven by oncogenic transformation). CHK1 is overexpressed and the ATR/CHK1 pathway is constitutively active in T-ALL, possibly triggered by RS. In turn, CHK1 limits the otherwise catastrophic amounts of RS capable of driving T-ALL cells into apoptosis. **(b)** Loss of CHK1 in T-ALL cells, either by pharmacologic inhibition or by gene knockdown, is accompanied by a deleterious rise of RS to levels that trigger apoptosis mediated, at least in part, by ATM and caspase-3.

not necessarily quiescent and instead display high levels of MYC,<sup>53</sup> which ignites cell cycle progression and frequently drives replication stress,<sup>54</sup> it is tempting to speculate that CHK1 inhibitors may preferentially target T-cell leukemia stem cells and therefore constitute effective tools for prevention of leukemia relapse.

In summary, our present studies constitute the first evidence that CHK1 is overexpressed and hyperactivated in T-ALL cells, displaying *de facto* an oncogene-like role in T-ALL by controlling excessive replication stress. Targeting CHK1 activity may be therefore a valid new therapeutic strategy against this malignancy.

## MATERIALS AND METHODS

### Primary samples, cell lines and culture

Primary T-ALL cells of pediatric patients at diagnosis and normal thymocytes were isolated as described in Silva *et al.*<sup>41</sup> In all cases, informed consent was obtained in accordance with the Declaration of Helsinki and under institutional ethical review board approval. When indicated, whole thymocytes were immunostained against CD3, CD4 and CD8 surface markers, as described in Silva *et al.*,<sup>55</sup> and CD3<sup>-</sup>CD4<sup>-</sup>CD8<sup>-</sup> triple-negative, CD4<sup>+</sup>CD8<sup>+</sup> double-positive and CD4 or CD8 single-positive sub-populations were isolated by cell sorting using FACSAria I or III (BD Bioscience, Madrid, Spain). The primary-like T-ALL cell line TAIL7 was established by our group.<sup>56</sup> All other T-ALL cell lines were obtained from a cell bank ([http://www.dsmz.de/human\\_and\\_animal\\_cell\\_line](http://www.dsmz.de/human_and_animal_cell_line)). Cell culture was conducted as before.<sup>41,55</sup> When indicated, hIL-7 (Peprotech EC, Rocky Hill, NJ, USA), CHK1 inhibitor PF-00477736 (Sigma, St Louis, MO, USA), ATR inhibitor ETP-46464 (obtained from Centro Nacional de Investigaciones Oncologicas, Madrid, Spain), ATM inhibitor KU55933 (Selleck Chemicals, Houston, TX, USA) or pancaspase inhibitor qVD-Oph (Sigma) were added. Vehicle (dimethylsulfoxide) controls were included in all experiments involving small-molecule inhibitors. For coculture experiments, T-ALL cells were seeded on a overnight grown OP9 (0.5 × 10<sup>6</sup> cells/cm<sup>2</sup>) stromal layer.

### Quantitative real-time PCR

*CHEK1* mRNA quantification was performed as described in Silva *et al.*<sup>41</sup> using the following primers: forward (5'-ATATGAAGCGTCCGTAGACT-3') and reverse (5'-TGCCTATGTCTGGCTCTATTCTG-3'), and normalized for the S18 transcript detected with the following primers: forward (5'-GGA GAGGGAGCCTGAGAAACG-3') and reverse (5'-CGCGGCTGCTGGCACCAG ACTT-3').

### Gene expression microarray analysis and unsupervised cluster analysis

The microarray data set of 117 T-ALL case samples has been previously described (GEO database, accession number GSE26713).<sup>14</sup> Unsupervised cluster analyses to assess differential expression of *CHEK1* within the T-ALL subgroups was performed using dChip as described.<sup>14</sup>

### *CHEK1* knockdown

Plasmids encoding lentiviruses expressing shRNAs were obtained from the RNAi Consortium.<sup>57</sup> The selected *CHEK1* shRNA (target sequence 5'-CCGGG TGGTTTATCTGCATGGTATTCTCGAGAATACCATGCAGATAAACCACTTTT-3'), validated by the RNAi Consortium as the best hairpin (98% knockdown) and the control hairpin (a scramble sequence against GFP) lentiviruses were produced as described previously.<sup>58</sup> Viral titers of 2.5–3.75 × 10<sup>7</sup>/ml, determined as in Barde *et al.*,<sup>59</sup> warranted a high efficiency of infection, avoiding puromycin selection. Jurkat cells were transduced by spin infection with polybrene and lentivirus (multiplicity of infection = 10) and viability was monitored daily thereafter.

### Immunoblotting

Immunoblots were performed as described in Silva *et al.*<sup>55</sup> with antibodies against poly (ADP-ribose) polymerase 1 (Novus, Cambridge, UK), P-RPA32 (S4/8) (Bethyl Laboratories, Montgomery, TX, USA), caspase-3, CDK1, CHK2, RPA32 and β-actin (Santa Cruz Biotechnology, Heidelberg, Germany) and P-ATR (S428), P-ATM (S1981), P-CHK1 (S317), P-CHK1 (S345), P-CHK1 (S296), CHK1, P-CHK2 (T68), P-CDK1 (Y15), CDC25C, caspase-2 and P-H2AX (S139) (all from Cell Signaling Technology, Leiden, The Netherlands).

### Cell viability and proliferation assessment

Cell viability was quantified by flow cytometry analysis of FSC × SSC distribution or by Annexin-V (eBioscience, Hatfield, UK) and 7-AAD (BD Biosciences, San Jose, CA, USA) double staining, as described.<sup>55</sup> Proliferation was assessed at the indicated times using alamarBlue (Life Technologies, Carlsbad, CA, USA) and fluorescence acquired using the Infinite 200 reader (Tecan, Männedorf, Switzerland) all according to the manufacturer's instructions.

### Cell cycle analysis

Propidium iodide staining was performed as described.<sup>13</sup> Percentages of diploid, tetraploid or replicating (2n–4n) live cells were determined by propidium iodide histogram gating using FlowJo (TreeStar, Ashland, OR, USA).

### Immunofluorescence

T-ALL cells (10<sup>5</sup>) cultured as indicated were collected, fixed in 3.7% formaldehyde and permeabilized with 0.1% Triton-X-100. Cells were then blocked with 0.05% Tween-20, 5% goat serum, incubated with anti-γH2AX antibody followed by incubation with goat anti-rabbit-TRITC (Molecular Probes, Carlsbad, CA, USA). Following 4',6-diamidino-2-phenylindole staining, cells were citospined, 'Slow-Fade' mounting medium (Invitrogen, Carlsbad, CA, USA) was added and images were acquired using a DMRA2 microscope (Leica, Wetzlar, Germany).

### *In vivo* human T-ALL model

Mice were housed and bred in a specific pathogen-free animal facility, treated in accordance with the EU guidelines and approval of the Institutional Ethical Committee. Eight-week-old non-obese diabetic/severe-combined immunodeficiency mice were subcutaneously injected in both flanks with 10<sup>7</sup> DND-4.1.Luciferase.GFP cells, generated as in Lonetti *et al.*<sup>60</sup> At day 5, tumor burden was assessed and mice were equally distributed into two groups to receive daily 10 mg/kg of PF-0047773 dissolved in 0.05 N sodium lactate, 5% manitol (pH 4.0) or vehicle by intraperitoneal injection. Mice were weighed frequently to determine treatment-induced toxicity. Tumor burden/growth was determined as in Lonetti *et al.*<sup>60</sup>

### Statistics

GraphPad Prism software (La Jolla, CA, USA) was used for statistical analysis. Differences between mean values were calculated using two-tailed Student's *t*-test and two-way analysis of variance, as appropriate. Differences were considered significant at *P* < 0.05.

## CONFLICT OF INTEREST

The authors declare no conflict of interest.

## ACKNOWLEDGEMENTS

This work was supported by the grant PTDC/SAU-ONC/113202/2009 from Fundação para a Ciência e a Tecnologia (FCT), Portugal. LMS, RN, IA, LRM and CM had postdoctoral fellowships, and VP a BI fellowship, all from FCT. We thank Dr J Ferreira for fruitful discussions and reagents. We also thank Dr O Fernandez-Capetillo and Centro Nacional de Investigaciones Oncologicas for providing the ATR inhibitor. We especially thank the generosity of patients and their families, and the collaboration of all the team from the Pediatrics Service of Instituto Português de Oncologia de Lisboa.

## REFERENCES

- 1 Pui CH, Robison LL, Look AT. Acute lymphoblastic leukaemia. *Lancet* 2008; **371**: 1030–1043.
- 2 Aifantis I, Raetz E, Buonamici S. Molecular pathogenesis of T-cell leukaemia and lymphoma. *Nat Rev Immunol* 2008; **8**: 380–390.
- 3 Gorgoulis VG, Vassiliou LV, Karakaidos P, Zacharatos P, Kotsinas A, Liloglou T *et al.* Activation of the DNA damage checkpoint and genomic instability in human precancerous lesions. *Nature* 2005; **434**: 907–913.
- 4 Bartkova J, Horejsi Z, Koed K, Kramer A, Tort F, Zieger K *et al.* DNA damage response as a candidate anti-cancer barrier in early human tumorigenesis. *Nature* 2005; **434**: 864–870.

- 5 Ferrando AA, Neuberger DS, Staunton J, Loh ML, Huard C, Raimondi SC *et al*. Gene expression signatures define novel oncogenic pathways in T cell acute lymphoblastic leukemia. *Cancer Cell* 2002; **1**: 75–87.
- 6 Mullighan CG, Goorha S, Radtke I, Miller CB, Coustan-Smith E, Dalton JD *et al*. Genome-wide analysis of genetic alterations in acute lymphoblastic leukaemia. *Nature* 2007; **446**: 758–764.
- 7 Weng AP, Ferrando AA, Lee W, Morris JP, Silverman LB, Sanchez-Irizarry C *et al*. Activating mutations of NOTCH1 in human T cell acute lymphoblastic leukemia. *Science* 2004; **306**: 269–271.
- 8 Sarmiento LM, Huang H, Limon A, Gordon W, Fernandes J, Tavares MJ *et al*. Notch1 modulates timing of G1-S progression by inducing SKP2 transcription and p27 Kip1 degradation. *J Exp Med* 2005; **202**: 157–168.
- 9 Dohda T, Maljukova A, Liu L, Heyman M, Grander D, Brodin D *et al*. Notch signaling induces SKP2 expression and promotes reduction of p27Kip1 in T-cell acute lymphoblastic leukemia cell lines. *Exp Cell Res* 2007; **313**: 3141–3152.
- 10 Zenatti PP, Ribeiro D, Li W, Zuurbier L, Silva MC, Paganin M *et al*. Oncogenic IL7R gain-of-function mutations in childhood T-cell acute lymphoblastic leukemia. *Nat Genet* 2011; **43**: 932–939.
- 11 Flex E, Petrangeli V, Stella L, Chiaretti S, Hornakova T, Knoops L *et al*. Somaticly acquired JAK1 mutations in adult acute lymphoblastic leukemia. *J Exp Med* 2008; **205**: 751–758.
- 12 Bains T, Heinrich MC, Loriaux MM, Beadling C, Nelson D, Warrick A *et al*. Newly described activating JAK3 mutations in T-cell acute lymphoblastic leukemia. *Leukemia* 2012; **26**: 2144–2146.
- 13 Barata JT, Cardoso AA, Nadler LM, Boussiotis VA. Interleukin-7 promotes survival and cell cycle progression of T-cell acute lymphoblastic leukemia cells by down-regulating the cyclin-dependent kinase inhibitor p27(kip1). *Blood* 2001; **98**: 1524–1531.
- 14 Homminga I, Pieters R, Langerak AW, de Rooi JJ, Stubbs A, Verstegen M *et al*. Integrated transcript and genome analyses reveal NKX2-1 and MEF2C as potential oncogenes in T cell acute lymphoblastic leukemia. *Cancer Cell* 2011; **19**: 484–497.
- 15 Lopez-Contreras AJ, Gutierrez-Martinez P, Specks J, Rodrigo-Perez S, Fernandez-Capetillo O. An extra allele of Chk1 limits oncogene-induced replicative stress and promotes transformation. *J Exp Med* 2012; **209**: 455–461.
- 16 Smith J, Tho LM, Xu N, Gillespie DA. The ATM-Chk2 and ATR-Chk1 pathways in DNA damage signaling and cancer. *Adv Cancer Res* 2010; **108**: 73–112.
- 17 Liu Q, Guntuku S, Cui XS, Matsuoka S, Cortez D, Tamai K *et al*. Chk1 is an essential kinase that is regulated by Atr and required for the G(2)/M DNA damage checkpoint. *Genes Dev*. 2000; **14**: 1448–1459.
- 18 Toledo LI, Murga M, Fernandez-Capetillo O. Targeting ATR and Chk1 kinases for cancer treatment: a new model for new (and old) drugs. *Mol Oncol* 2011; **5**: 368–373.
- 19 Zhang Y, Hunter T. Roles of Chk1 in cell biology and cancer therapy. *Int J Cancer* 2013; **134**: 1013–1023.
- 20 Mailand N, Falck J, Lukas C, Syljuasen RG, Welcker M, Bartek J *et al*. Rapid destruction of human Cdc25A in response to DNA damage. *Science* 2000; **288**: 1425–1429.
- 21 Syljuasen RG, Sorensen CS, Hansen LT, Fugger K, Lundin C, Johansson F *et al*. Inhibition of human Chk1 causes increased initiation of DNA replication, phosphorylation of ATR targets, and DNA breakage. *Mol Cell Biol* 2005; **25**: 3553–3562.
- 22 Katsuno Y, Suzuki A, Sugimura K, Okumura K, Zineldeen DH, Shimada M *et al*. Cyclin A-Cdk1 regulates the origin firing program in mammalian cells. *Proc Natl Acad Sci USA* 2009; **106**: 3184–3189.
- 23 Petermann E, Woodcock M, Helleday T. Chk1 promotes replication fork progression by controlling replication initiation. *Proc Natl Acad Sci USA* 2010; **107**: 16090–16095.
- 24 Lopes M, Cotta-Ramusino C, Pelliccioli A, Liberi G, Plevani P, Muzi-Falconi M *et al*. The DNA replication checkpoint response stabilizes stalled replication forks. *Nature* 2001; **412**: 557–561.
- 25 Sorensen CS, Hansen LT, Dziegielewska J, Syljuasen RG, Lundin C, Bartek J *et al*. The cell-cycle checkpoint kinase Chk1 is required for mammalian homologous recombination repair. *Nat Cell Biol* 2005; **7**: 195–201.
- 26 Lam MH, Liu Q, Elledge SJ, Rosen JM. Chk1 is haploinsufficient for multiple functions critical to tumor suppression. *Cancer Cell* 2004; **6**: 45–59.
- 27 Zaugg K, Su YW, Reilly PT, Moolani Y, Cheung CC, Hakem R *et al*. Cross-talk between Chk1 and Chk2 in double-mutant thymocytes. *Proc Natl Acad Sci USA* 2007; **104**: 3805–3810.
- 28 Verlinden L, Vanden Bempt I, Eelen G, Drijckoningen M, Verlinden I, Marchal K *et al*. The E2F-regulated gene Chk1 is highly expressed in triple-negative estrogen receptor/progesterone receptor/HER-2 breast carcinomas. *Cancer Res* 2007; **67**: 6574–6581.
- 29 Xu J, Li Y, Wang F, Wang X, Cheng B, Ye F *et al*. Suppressed miR-424 expression via upregulation of target gene Chk1 contributes to the progression of cervical cancer. *Oncogene* 2013; **32**: 976–987.
- 30 Cole KA, Huggins J, Laquaglia M, Hulderman CE, Russell MR, Bosse K *et al*. RNAi screen of the protein kinome identifies checkpoint kinase 1 (CHK1) as a therapeutic target in neuroblastoma. *Proc Natl Acad Sci USA* 2011; **108**: 3336–3341.
- 31 Carrassa L, Damia G. Unleashing Chk1 in cancer therapy. *Cell Cycle* 2011; **10**: 2121–2128.
- 32 Toledo LI, Murga M, Zur R, Soria R, Rodriguez A, Martinez S *et al*. A cell-based screen identifies ATR inhibitors with synthetic lethal properties for cancer-associated mutations. *Nat Struct Mol Biol*. 2011; **18**: 721–727.
- 33 Zou L, Elledge SJ. Sensing DNA damage through ATRIP recognition of RPA-ssDNA complexes. *Science* 2003; **300**: 1542–1548.
- 34 Liu S, Opiyo SO, Manthey K, Glanzer JG, Ashley AK, Amerin C *et al*. Distinct roles for DNA-PK, ATM and ATR in RPA phosphorylation and checkpoint activation in response to replication stress. *Nucleic Acids Res* 2012; **40**: 10780–10794.
- 35 Forment JV, Blasius M, Guerini I, Jackson SP. Structure-specific DNA endonuclease Mus81/Eme1 generates DNA damage caused by Chk1 inactivation. *PLoS ONE* 2011; **6**: e23517.
- 36 Gagou ME, Zuazua-Villar P, Meuth M. Enhanced H2AX phosphorylation, DNA replication fork arrest, and cell death in the absence of Chk1. *Mol Biol Cell* 2010; **21**: 739–752.
- 37 Zhang YW, Brognard J, Coughlin C, You Z, Dolled-Filhart M, Aslanian A *et al*. The F box protein Fbx6 regulates Chk1 stability and cellular sensitivity to replication stress. *Mol Cell* 2009; **35**: 442–453.
- 38 Sidi S, Sanda T, Kennedy RD, Hagen AT, Jette CA, Hoffmans R *et al*. Chk1 suppresses a caspase-2 apoptotic response to DNA damage that bypasses p53, Bcl-2, and caspase-3. *Cell* 2008; **133**: 864–877.
- 39 Myers K, Gagou ME, Zuazua-Villar P, Rodriguez R, Meuth M. ATR and Chk1 suppress a caspase-3-dependent apoptotic response following DNA replication stress. *PLoS Genet* 2009; **5**: e1000324.
- 40 Scupoli MT, Perbellini O, Krampera M, Vinante F, Cioffi F, Pizzolo G. Interleukin 7 requirement for survival of T-cell acute lymphoblastic leukemia and human thymocytes on bone marrow stroma. *Haematologica* 2007; **92**: 264–266.
- 41 Silva A, Laranjeira AB, Martins LR, Cardoso BA, Demengeot J, Yunes JA *et al*. IL-7 contributes to the progression of human T-cell acute lymphoblastic leukemias. *Cancer Res* 2011; **71**: 4780–4789.
- 42 Ribeiro D, Melao A, Barata JT. IL-7R-mediated signaling in T-cell acute lymphoblastic leukemia. *Adv Biol Regul* 2013; **53**: 211–222.
- 43 Sarmiento LM, Barata JT. Therapeutic potential of Notch inhibition in T-cell acute lymphoblastic leukemia: rationale, caveats and promises. *Expert Rev Anticancer Ther* 2011; **11**: 1403–1415.
- 44 Indraccolo S, Minuzzo S, Masiero M, Pusceddu I, Persano L, Moserle L *et al*. Cross-talk between tumor and endothelial cells involving the Notch3-Dll4 interaction marks escape from tumor dormancy. *Cancer Res* 2009; **69**: 1314–1323.
- 45 Brooks K, Oakes V, Edwards B, Ranall M, Leo P, Pavey S *et al*. A potent Chk1 inhibitor is selectively cytotoxic in melanomas with high levels of replicative stress. *Oncogene* 2013; **32**: 788–796.
- 46 Niida H, Tsuge S, Katsuno Y, Konishi A, Takeda N, Nakanishi M. Depletion of Chk1 leads to premature activation of Cdc2-cyclin B and mitotic catastrophe. *J Biol Chem* 2005; **280**: 39246–39252.
- 47 Castedo M, Perfettini JL, Roumier T, Andreau K, Medema R, Kroemer G. Cell death by mitotic catastrophe: a molecular definition. *Oncogene* 2004; **23**: 2825–2837.
- 48 Ma CX, Janetka JW, Piwnicka-Worms H. Death by releasing the breaks: CHK1 inhibitors as cancer therapeutics. *Trends Mol Med* 2011; **17**: 88–96.
- 49 Sugimoto K, Sasaki M, Isobe Y, Tsutsui M, Suto H, Ando J *et al*. Hsp90-inhibitor geldanamycin abrogates G2 arrest in p53-negative leukemia cell lines through the depletion of Chk1. *Oncogene* 2008; **27**: 3091–3101.
- 50 Dai Y, Rahmani M, Pei XY, Khanna P, Han SI, Mitchell C *et al*. Farnesyltransferase inhibitors interact synergistically with the Chk1 inhibitor UCN-01 to induce apoptosis in human leukemia cells through interruption of both Akt and MEK/ERK pathways and activation of SEK1/JNK. *Blood* 2005; **105**: 1706–1716.
- 51 Zhang C, Yan Z, Painter CL, Zhang Q, Chen E, Arango ME *et al*. PF-00477736 mediates checkpoint kinase 1 signaling pathway and potentiates docetaxel-induced efficacy in xenografts. *Clin Cancer Res* 2009; **15**: 4630–4640.
- 52 Brown EJ, Baltimore D. ATR disruption leads to chromosomal fragmentation and early embryonic lethality. *Genes Dev* 2000; **14**: 397–402.
- 53 King B, Trimarchi T, Reavie L, Xu L, Mullenders J, Ntziachristos P *et al*. The ubiquitin ligase FBXW7 modulates leukemia-initiating cell activity by regulating MYC stability. *Cell* 2013; **153**: 1552–1566.
- 54 Murga M, Campaner S, Lopez-Contreras AJ, Toledo LI, Soria R, Montana MF *et al*. Exploiting oncogene-induced replicative stress for the selective killing of Myc-driven tumors. *Nat Struct Mol Biol* 2011; **18**: 1331–1335.
- 55 Silva A, Yunes JA, Cardoso BA, Martins LR, Jotta PY, Abecasis M *et al*. PTEN posttranslational inactivation and hyperactivation of the PI3K/Akt

- pathway sustain primary T cell leukemia viability. *J Clin Invest* 2008; **118**: 3762–3774.
- 56 Barata JT, Boussiotis VA, Yunes JA, Ferrando AA, Moreau LA, Veiga JP *et al*. IL-7-dependent human leukemia T-cell line as a valuable tool for drug discovery in T-ALL. *Blood* 2004; **103**: 1891–1900.
- 57 Moffat J, Grueneberg DA, Yang X, Kim SY, Kloepfer AM, Hinkle G *et al*. A lentiviral RNAi library for human and mouse genes applied to an arrayed viral high-content screen. *Cell* 2006; **124**: 1283–1298.
- 58 Real G, Monteiro F, Burger C, Alves PM. Improvement of lentiviral transfer vectors using cis-acting regulatory elements for increased gene expression. *Appl Microbiol Biotechnol* 2011; **91**: 1581–1591.
- 59 Barde I, Salmon P, Trono D. Production and titration of lentiviral vectors. *Curr Protoc Neurosci* 2010; **53**: 4.21.1–4.21.23.
- 60 Lonetti A, Antunes IL, Chiarini F, Orsini E, Buontempo F, Ricci F *et al*. Activity of the pan-class I phosphoinositide 3-kinase inhibitor NVP-BKM120 in T-cell acute lymphoblastic leukemia. *Leukemia* 2013; **28**: 1196–1206.

Supplementary Information accompanies this paper on the Oncogene website (<http://www.nature.com/onc>)